Earth Surface Processes and Landforms

The role of GPR techniques in determining ice cave properties: Peña Castil ice cave, Picos de Europa.

Journal:	*Earth Surface Processes and Landforms*
Manuscript ID	ESP-16-0066.R2
Wiley - Manuscript type:	Paper
Date Submitted by the Author:	n/a
Complete List of Authors:	Gómez-Lende, Manuel; Valladolid, Geography Cañadas, Enrique; Universidad de Valladolid, Geografía Bordehore, Luis; Facultad de Ingeniería en Ciencias de la Tierra, Escuela Superior Politécnica del Litoral, ESPOL Sandoval, Senén; Geofísica Consultores, Torrelodones
Keywords:	ground-penetrating radar, ice cave, ice block, internal structure, Picos de Europa

The role of GPR techniques in determining ice cave properties: Peña Castil ice cave, Picos de Europa.

Manuel Gómez Lende[a]*, Enrique Serrano Cañadas[b], Luis Jordá Bordehore[b], Senén Sandoval[c].

[a] University of Valladolid. GIR PANGEA, Dpt. Geografía, Paseo Prado de la Magdalena s/n, 47011 Valladolid, Spain.

[b] Escuela Superior Politécnica del Litoral, ESPOL, Facultad de Ingeniería en Ciencias de la Tierra, Campus Gustavo Galindo Km 30.5 Vía Perimetral, P.O. Box 09-01-5863, Guayaquil, Ecuador

[c] Geofísica Consultores S.L. Calle Ricardo León, 33, 28250 Torrelodones, Madrid, Spain.

* Corresponding author. Email addresses: manuelglende@hotmail.com, serranoe@fyl.uva.es, ljorda@espol.edu.ec, senen@geofisica-consultores.es

ABSTRACT: The structure and ice content of ice caves are poorly understood. Ground Penetrating Radar (GPR) can provide useful insights but has only rarely been applied to ice caves. This paper interprets GPR images (radargrams) in terms of internal structure, stratification, compaction, thickness and volume of the ice block in the Peña Castil ice cave (Central Massif of Picos de Europa, Northern Spain), providing the endokarst geometry of the ice cave in GPR data reflections. Eight radargrams were obtained by applying a shielded ground-coupled antenna with a nominal frequency of 400 MHz. Although the radargrams do not depict the ice-basal bedrock interface, they suggest that the ice block is at least 54m deep and similarly thick. Some curved reflection signatures suggest a potential vertical displacement in the block of ice, and thus

certain dynamics in the ice body. Other images show numerous interbedded clasts and thin sediment layers imaged as banded reflections. In this particular cave a direct visual inspection of the ice stratigraphy is a difficult task but GPR provides clear reflectivity patterns of some of its internal features, making GPR a suitable instrument for this and future studies to achieve a better and broader understanding of the internal behavior of ice caves.

KEYWORDS: ground-penetrating radar, ice cave, ice block, internal structure, Picos de Europa

Introduction

Ice caves can be defined as natural karstic cavities in which a perennial ice mass is preserved deriving from the metamorphism of accumulated snow and/or freezing water within it (filtered from outside or from internal melting of cryomorphologies). These caves have specific karst pattern and climatic conditions which, together with certain water and air circulations, mean that ice accumulations are preserved inside them forming stratified ice blocks (perennial cave ice) and cryospeleothems (generally seasonal and non-stratified morphologies).

The attention of the scientific community and the importance given to ice caves is the result of the potential to make paleoclimatic reconstructions of what their ice blocks enclose. This relevance has recently been made clear on many occasions, thanks mainly to isotopic analysis of ice (e.g. Fórizs *et al.*, 2004. 2006; Viehmann *et al.*, 2004; Kern *et al.*, 2004, 2006, 2008; Luetscher, 2005; Holmlund *et al.*, 2005; Filipov, 2005; Citterio *et al.*, 2005; Vrana *et al.*, 2006;

Clausen *et al.*, 2006; Stoffel *et al.*, 2009; Feurdean *et al.*, 2011; Perşoiu *et al.*, 2011; May *et al.*, 2011; Maggi *et al.*, 2012; Sancho *et al.*, 2012); and even more recently to the geochemical studies of cryogenic calcites (e.g. Lauriol and Clark, 1993; Dickfoss, 1996; Žák *et al.*, 2004, 2008; Lacelle, 2007; Lacelle *et al.*, 2009; Richter and Riechelmann, 2008; Richter *et al.*, 2010; Luetscher *et al.*, 2013; Spötl and Cheng, 2014).

This, together with an age that may be as much as thousands of years (e.g. 5516±70 cal BP in "A294 ice cave" (Central Pyrenees - Sancho *et al.*, 2012), or 5180±130 BP in "Eisgruben-Eishöhle" (Sarstein, Austrian Alps, - Achleitner, 1995) makes this periglacial phenomenon a powerful instrument for the reconstruction of recent paleoenvironments to complement the usual information sources. In this sense, the paleoclimatic records of the ice cave take on particular importance in mid and low-altitude environments in which there is no surface ice (e.g. Glacière de Monlési - Luetscher, 2005; Mammuthöhle - Kern *et al.*, 2011; Vukušic Ice Cave - Kern *et al.*, 2011b; Eisriesenwelt - May *et al.*, 2011; or Scărişoara-Perşoiu, 2011), or in completely deglaciated high mountain areas, as is the case of Picos de Europa (Gómez-Lende, 2015).

In spite of this importance and its being a phenomenon present and known in many parts of the world, scientific disciplines have paid little attention to ice caves, among other reasons because of how modestly representative they are in the context of ice volumes on a planetary scale. This has led to their being the least known element in the cryosphere today (Kern and Perşoiu, 2013) in spite of the intensification in efforts to study them in recent decades.

Added to this demand for greater attention is the fact that in general most ice caves studied to date present a pronounced ice mass loss trend worldwide

(Kern and Perşoiu, 2013), which makes greater knowledge of ice caves necessary and urgent from several perspectives and using all instruments available in order to better understand them and to be able to obtain their maximum paleoclimatic potential before many of them disappear. One such instrument is the Ground Penetrating Radar (GPR).

GPR studies in ice caves

Due to its relative ease of use on site -it covers relatively large areas in a reasonably short time, its non-invasive nature and the fact that modern equipment can collect and process a lot of data relatively easily-, we find many radar studies of glaciers and permafrost, and its usefulness as a technique for surveying thicknesses and anomalies is widely agreed (Navarro *et al.*, 2009; Arcone, 1996; Travassos and Simoes, 2004; Fukui *et al.*, 2007). The morphology of permafrost and glacial ice differs considerably from that of ice caves, and even taking into account on the analysis of these media, the ice caves research has been centered exclusively on the application of the georadar to the type of ice.

The usefulness of GPR as a tool in the study of ice blocks within ice caves has been demonstrated in previous studies (e.g. Hausmann and Behm, 2011). It facilitates the measurement of different parameters fundamental to the internal structure, which is why it has been used in the present study. It indicates the degree of melting and the weakness of an ice block, offering details, often not visible, of its compaction, and with it attempt to predict its evolution in the near future. It also permits us to know the degree of stratification and then interpret the polygenetic nature of the ice block, as well as the greater or lesser quantity

of clasts within it. This, together with the lie of the strata, helps us to determine internal flows and deformities to which the block is subjected, and therefore to interpret the origin, behavior and future evolution of the ice. Determining the geometry of the cavity and the volumes and thickness of the ice block is also possible through the application of GPR. And all of this can serve to select the best place in the ice block to carry out later research in order to go deeper into its paleoclimatic potential (e.g. drilling).

Nowadays geophysical techniques for the study of ice blocks in ice caves have seldom been used. In the majority of cases the aim has been the quantification of volumes (Geczy and Kucharovi, 1995; Novotný and Tulis, 1995; Behm and Hausmann, 2007; Podsuhin and Stepanov, 2008; Colucci *et al.*, 2012; Rojšek, 2012; Stepanov *et al.*, 2014; Garašić, 2014), whereas in others they have been of use in finding the largest ice thicknesses prior to drilling cores (Kern *et al.*, 2011; Colucci *et al.*, 2014). On just a few occasions they have been used for the analysis of the internal structure of the block or to determine cave geometries (Behm and Hausmann, 2008; Behm *et al.*, 2010; Hausmann and Behm, 2011). Also, GPR data have been acquired on ice blocks inside caves with the aim of checking the applicability of this technique in searching for underground water or ice on Mars (Ciarletti *et al*, 2013a, 2013b).

In the Iberian Peninsula, ice cave studies are very recent. The only ice caves that have been studied scientifically are in the Pyrenees (Belmonte and Sancho, 2010; Belmonte *et al.*, 2011, 2012, 2014, Sancho *et al.*, 2014; Leunda *et al.*, 2015); and Picos de Europa (Gómez-Lende *et al.*, 2011, 2014; Berenguer *et al.*, 2014; Gómez-Lende 2015; Gómez-Lende and Serrano, 2012a, 2012b, 2012c, 2013, 2014), however none of these studies involved the application of GPR.

Difficulty of access acts as a deterrent to scientific fieldwork applying electric or electromagnetic geophysical techniques in caves which have, nevertheless, been successfully applied in other periglacial studies on the surface in Picos de Europa, for example (Del Río *et al.*, 2009; Serrano *et al.*, 2010, 2011; Paniagua *et al.*, 2004; Serrano *et al.*, 2012)

With the aim of improving knowledge of the internal structure and thickness of the ice block, which permits the interpretation of the current state of the ice, its organization and its evolution in the near future as well as determining possible places suitable for carrying out future research, in the present study we applied GPR to the ice block of the Peña Castil ice cave (Picos de Europa).

Study Area and Cave Setting

The Peña Castil ice cave is located in the high periglacial mountain environment of the Picos de Europa, an Atlantic glaciokarst high mountain in the north of the Cantabrian Range (northern Spain) with a maximum altitude of 2648 m.a.s.l. (Torrecerredo) (Figure 1). Actually, this high mountain environment is a marginal periglacial and totally deglaciated landscape in which perennial ice bodies remain at the surface (perennial snow and ice patches from the glaciers of the Little Ice Age) and below it (ice caves).

The cave studied is located in the Central Massif of the Picos de Europa (43º1'21"N/4º47'48"W), under the Peña Castil summit (2444 m.a.s.l.) and hanging over the Duje valley (Figure 1). The lower and main entrance is located at 2095 m.a.s.l. with an eastern orientation without other entrances worth consideration. Speleological surveys have not revealed any other lower entrances, although the cave morphology suggests minor upper entrances

(Figure 2). The horizontal development is around 65 m and the vertical is still unknown (currently -84 m). The entrance comprises an “Entrance ramp” (snowy entrance slope; sector 1) leading to two main “Ice rooms” (“Lower room” and “Upper room”; sectors 2 and 3) in which the ice body is located, and a small “Terminal room” (sector 5) after passing through a narrow “Corridor” (sector 4). Neither the “Corridor” and “Terminal room” have perennial ice. There is a small “Filling shaft” that can be accessed from the “Lower room” by descending a narrow ramp.

The perennial ice deposit at the surface is about 629 m^2 and its thickness, as far as is known to date, is at least 54 m (the basal bedrock interface is unknown). It involves an estimated ice filling of at least 33.300 m^3 (Gómez Lende, 2015). The air temperature inside is constant throughout the summer period and irregular during the winter period; however the annual average is below 0ºC (Gómez-Lende *et al.*, 2014) (Table I). According to glacioclimatological criteria (Luetscher and Jeannin, 2004) it is a static ice cave with firn and congelation ice (Gómez-Lende, 2015).

Method

This study is based on speleological explorations made in 2011 (Sánchez *et al.*, 2011) and GPR surveys carried out in August 2014. Data acquisition was achieved with a shielded ground-coupled antenna manufactured by IDS (Ingenieria dei Sistemi) with a nominal frequency of 400 MHz (Figure 3). The transmitter (Tx) and receiver (Rx) elements are embedded in a common casing allowing data to be gathered by the common-offset method. The software used

to acquire the data was IDS-K2. To process raw signals GRESWINv1 (IDS-Spa, 2005) was used.

During fieldwork, different time window lengths (data time windows in which underground reflections are collected) were used: 120 ns, 160 ns, 320 ns and 1280 ns with a variable number of samples between 512 and 4096. It is worth pointing out that 1 ns (10-9 s) is the time needed by light to travel 30 centimetres (in a vacuum), thus the precision of measurements is very high. A window length of 120 ns with 512 samples was selected for the majority of the profiles shown in this work.

The GPR survey was carried out using a 400 MHz antenna, commonly used in alpine ice caves (Hausmann and Behm, 2011). This makes a good compromise between resolution and depth of penetration, given that in general the lower frequency antennas are those that reach greater depth with lower resolution. On the other hand, the higher frequency radar antennas (in the range of 800 MHz – 2 GHz) penetrate less but with better definition. The antennas of 200 to 600 MHz are those most commonly used in mixed studies of similar characteristics to the present one. Such is the case of glaciers in which, among other things, snow cover and basal bedrock thicknesses are measured, although there are references to antennas of lower resolution and greater penetration, such as 50 MHz (Travassos and Simoes, 2004) or 20MHz - 200MHz (Navarro *et al.*, 2009).

Data were acquired along eleven profiles on the surface of the ice block (profiles 1-11), but three profiles were rejected due to a lack of resolution (profiles 7, 8 and 11): profiles 1 to 6 in “lower room” and profiles 9 and 10 in “upper room”. Figure 4 shows the results of applying radar time windows

between 120 ns and 320 ns, and using standard physical parameters of ice proposed by previous authors (Hubbard and Glasser, 2005) (Table II).

Results

Pattern analysis of GPR profiles

All the radargrams show different layering patterns and reflection intensities, on a marked and repetitive banding that can be seen in all the profiles and at all depths.

In most of the radargrams two large reflection patterns can be generically distinguished with very distinctive sharpness (Figure 4):

- “Pattern A” presents a sub-horizontal or slightly concave layering, continuous along a good part of profiles (pattern A in Figure 4). It is characterized by its relative homogeneity in the return signals, weak in its reflection, sporadically sharp and differently orientated. Reflection hyperbolae are also common, forming high amplitude features spaced randomly across the radargrams with a more intense reflection than the surrounding signals (a.1 in Figure 4).

- “Pattern B” is defined by intense reflectivity characterized by very closely spaced hyperbolae (pattern B in Figure 4), in which the sub-horizontal banding is not clearly visible. Abrupt changes in electromagnetic properties explain the presence of hyperbolae and are characteristic of this pattern. They also show up randomly spread and as very highly energetic hyperbolae, though only in some profiles (e.g, profile 2 in Figure 4).

Pattern A shows reflection signals of lesser intensity and greater homogeneity with respect to the reflections of pattern B, in which the reflections are more chaotic and irregular, but sharper.

Pronounced reflection signatures are observed in all the radargrams. These signatures reveal particularly intense diffractions down to one metre depth from the surface (although in some profiles they appear at greater depths and with lesser wave intensities; see profiles 1, 2, 3 and 9), or reflections that are prolonged at greater depths (see profiles 1, 2, 3, 4 and 9).

In addition to these reflection hyperbolae, in all the “Lower room” radargrams, parallel straight-line signals at different depths are seen with good intensity (yellow arrows in the profiles from 1 to 6, Figure 4). As they do not present diffraction hyperbolae they correspond to continuous, homogeneous reflectors. They form a continuity in the reflected trace with an appreciable slope towards the centre of the profiles (the centre of the “Lower room”). In some of the profiles these signals form a broad arch that crosses the entire surveyed surface (profile 2). In most cases the signal is blurred at depth due to the profusion of the previously mentioned hyperbolae. The abovementioned signals are not reflected, however, in the “Upper room” (profiles 9 and 10).

In the upper part (the first nanoseconds of GPR reflections) all radargrams exhibit reflections down to depths of around 10-20 cm. These features have not been completely eliminated by filtering. A more careful inspection reveals areas with parallel and perfectly horizontal reflection bands down to a depth of one metre, which introduces a strong interference between the shallow waves and the rest of the ice body surveyed (green boxes in Figure 4).

Other reflections with different characteristics were found. On one hand, there are low amplitude hyperbolae, similar to those described earlier but located in the central parts of the room and of lesser amplitude, and on the other hand

there are intense hyperbolic reflections, located deeper (Figures 6 and 7 respectively).

Interpretation

Thickness and volume of ice mass

The bedrock at the bottom of the cave cannot be observed sharply in the radargrams and thus, neither could a thickness of the ice block be determined. All the profiles show a continuity of the ice block to at least 7 m depth, without noteworthy differences in thickness. Changes were not found in the reflection signatures as a result of the ice-basal bedrock interface in any of the cases, which indicates the vertical continuity of both the ice block and the cave.

Cave geometry

In the GPR profiles clear changes are observed in the reflections at the margins of the “Ice room”, corresponding to the sharp hyperbolae aligned in a vertical trace (B in Figure 4). According to the sections where they are found in each radargram and depending on the geometry of the cavity, we interpret them as the back reflections produced by the contact of the ice block with the end of the snow ramp entrance (profiles 1 to 4, Figure 5). The accumulation of clasts in the first strata (appreciated on the ground by visual inspections) could lead to many sharp reflection hyperbolae. Underneath, there are reflective signatures at the ends of nearly all profiles that do not correspond to the ice block (profiles 1, 2, 3, 4 and 5 in Figure 5 for the “Lower room” and profile 9 in Figure 5 for the “Upper room”). These reflections can be interpreted as the basal bedrock of the cave. This correspondence with the ice-bedrock interface extends deeper revealing the possible vertical geometry of the cave. In this case, the ice block could fill a vertical shaft, which is coherent with the prevailing endokarstic

morphologies in the Picos de Europa and with the ice filling in other ice caves in these mountains (Gómez-Lende, 2015).

Internal structure

The reflection signatures with very acute angles and of smaller amplitudes located in the central areas of the "Lower room" may be caused by boulders embedded within the ice block both in the surface layers and in the lower strata (where the signals are fainter), as described in other cave ice GPR studies (Hausmann and Behm, 2011; Colucci *et al*., 2014).

The origin of strong individual hyperbolae at greater depth is more difficult to determine. Their abundance from 2-3 m depth in almost all the profiles and the sharpness of their reflection signal has two possible origins:

- The presence of internal tunnels in the ice block like those observed descending to 15 m below the surface of the block (Gómez-Lende *et al*., 2014). These tunnels may or not be filled with congelation ice. These individual and broad hyperbolae have previously been interpreted as the reflection of intraglacial tunnels in glaciers (e.g. Moorman and Michel, 2000).

- The existence of numerous interbedded boulders. This hypothesis seems the most likely given that, in the former case, if the tunnels were filled with congelation ice or if they were air-filled cavities (Figure 7) a significant change in the reflected waves below the hyperbolae would be expected.

Banded layering is reflected in the first metres of the radargrams. These reflections occur at depth along a parallel-subparallel plane. One of these reflections shows slight undulations with different amplitudes within the ice block (profile 2 in Figure 9). We attribute the different sharpness in its reflection to the different sedimentary content of the strata. Those strata with greater content in

cryogenic calcite produce a sharper signal return. These are fine sediments, since clasts may generate a more irregular signal with more acute reflection hyperbolae. This consideration is coherent with the observation during the speleological exploration of different cryogenic calcite contents in adjacent strata (Figure 8).

Ciarletti *et al*. (2013b) attributed similar reflection signatures to internal fractures in the ice block. In this case, however, these prominent reflection waves in the upper part of the radargrams are not interpreted as internal fractures of the ice block due to their parallel orientation with respect to the stratification of the upper part of the radargrams. Although they sometimes appear oblique to the rest of the strata, this is not in contradiction with the proposed origin, as in this case they correspond to marked sedimentation hiatuses in the cave ice stratigraphy (black circle in Figure 8), as in the case of alpine ice caves (Colucci *et al*., 2014) and other ice caves in Picos de Europa currently under study (Altáiz and Verónica ice caves, Sánchez *et al*., 2011; Gómez-Lende *et al*., 2011).

The remaining continuous and less energetic reflections, parallel or sub-parallel to the previous ones, characterize the first metres of all radargrams, and at some specific sections they reach greater depths. We observe how these lines and the previous ones draw successive broad arches, curved in the central parts of the “Lower room” (profile 2 in Figure 9). These structures could be reflected by cave ice stratification and its deformation towards the central areas due to the shaft-shaped configuration previously mentioned and to the gravitational displacement of the ice mass accompanied by the potential melting or weakening of the ice block at its base.

In the upper parts (first centimetres from the surface) congelation ice layers are identified in agreement with field observations. All radargrams show that from 20 cm depth the reflection pattern is homogenous throughout the ice block, except where there are surface clasts, and in the possible contact between the ice block and the "entrance ramp" (bedrock interface). At some sections parallel bands with reversed polarity appear (green squares in Figure 10). These features can be interpreted as melting morphologies (melting channels, shallow melting ponds, etc.) on the surface of the ice block, later filled with congelation ice, which can reach over a metre in depth, as both radargrams and photographs reveal (Figure 10).

Ice mass compaction

If the broad reflection hyperbolae correspond to large embedded clasts, and not to internal tunnels or cryokarst cavities, the ice block can be considered, at least to the depths surveyed, to be a compact ice mass (no ablation morphologies are appreciated). The superficial fissures visible in some seasons of the year (melting periods in summer and autumn months) are not reflected in the interpreted profiles. In this way, considering that in the first 5-6 m depth of certain parts of the ice block hyperbolae that reflect the presence of clasts are absent suggests that the ice block forms a single-unit homogeneous mass in the first 7 m of its thickness (Figure 11).

Discussion

Behm and Hausmann (2007) applied different GPR frequencies (200, 400, 600 and 1200 MHz) using shielded antennae and with recording time windows ranging between 100 and 400 ns, obtaining high quality results. Following their

methodology and in view of the results they obtained, we directly used 400 MHz antennae, given that they provide a good compromise between resolution and depth, with signal acquisition time windows of 120 ns. The results are very promising, as determined by the quality of the data gathered for the study of the ice block in the ice cave.

Behm and Hausmann (2007) attributed the intense reflection bands at the base of the ice block to the abundance of thin sediments or liquid water content in the ice-bedrock interface, and the banding of its radargrams to the alternation of thin sediments (Behm and Hausmann, 2007; Hausmann and Behm, 2011). We cannot conclude that the different strata distinguished in the cave radargrams are produced by differences in the sedimentary content or to the different compositions of air bubbles due to the impossibility of making a direct observation of the strata. Nevertheless, its origin can be inferred as being a consequence of the different thin sediment content (cryogenic calcite) extrapolating the observations made of the ice block during speleological fieldwork. The reflection bands, therefore, may correspond to ice block stratification, ice layers alternating with thin sediments and cryogenic calcite layers. This is consistent with our visual observations during speleological fieldwork and studies in other ice caves (Hausmann and Behm, 2011).

The GPR survey did not enable us to determine the depth of the ice block, nor to establish the ice-basal bedrock interface, which would suggest the real thickness of the ice mass. Speleological explorations reveal that the ice block might have a mean thickness of as much as 54 m (GELL, 1995), which would yield a volume of at least 33,000 m^3. What has been established, however, is the underneath morphology of the cavity as a shaft of large dimensions and with

a high degree of verticality (ice-lateral bedrock interface in some radargram sections) down to a depth of 7 m. The main shaft would be found behind the entrance ramp, occupying entirely the “Ice room”, where the ice block is located. The thickness interpretation estimated, 7 metres depth of radargram signal, is coherent with the 54 m minimum ice block thickness suggested in explorations and topo-speleological studies (GELL, 1995; Sánchez *et al*., 2011, Gómez-Lende *et al*., 2012).

This is an ice block with a possible compact mass and sub-horizontal concave stratification, in which ice strata and strata with greater cryogenic calcite contents may alternate, as well as scattered and interbedded clasts. The curved signal of the strata, their disposition throughout the profiles and their continuity at depth suggest a deformation of the ice mass deriving from possible vertical gravitational displacement depending on the configuration of the shaft, with a potential basal melting of the ice block in the ice-basal bedrock interface (causing the downward movement of the ice block). This is the current situation of the blocks of nearby ice caves such as Altáiz, where intense basal melting has left the ice block completely suspended around 30 m over the base of the chasm, held up only by the shaft walls (Sánchez *et al*., 2011; Gómez-Lende *et al*., 2011; Gómez-Lende, 2015). Deformation by basal melting has been observed in many other ice caves (e.g. Citterio *et al*., 2003), with acceleration processes of basal melting due to the presence of air dynamics that circulate between the ice and rock (e.g. Kern *et al*., 2008).

In case of the two main types of reflection hyperbolae distinguished, we can interpret in two ways. On the one hand, in the case of the hyperbolae with arches of broad curvature, they are the scattered back reflections produced by

internal clasts, ruling out possible tunnels or internal cryocaves. On the other hand, the reflection hyperbolae are interpreted as features produced by superficial embedded clasts in the ice block, which may be seen in the first 50-100 cm of the congelation ice strata. It is consistent with the quantity of gravitational debris observed both in certain sub-surface sectors of the congelation ice in the ice block, as in the rooms immediate to the "Ice room" ("Corridor" or "Terminal Room"). Despite the fact that no boulders or clasts have been observed at the surface we can consider that the existence of internal boulders or clasts in the Peña Castil ice block is very probable due to the presence of these noticeable broad angle hyperbolae. The presence of embedded clasts in the ice block has been confirmed in field observations made in other ice caves in Picos de Europa (e.g. Verónica ice cave, Sánchez *et al*., 2011; Gómez-Lende *et al*., 2011). Similar reflection hyperbolae have been interpreted as clasts buried in ice bodies (e.g. Hausmann and Behm, 2011; Colucci et al., 2014), and in geo-cryological near cases such as the Jou Negro ice patch (in Picos de Europa surface, Del Río *et al*., 2009).

In the superficial strata there are reversed-polarity reflection bands compared to reflections from adjacent strata. They are interpreted as congelation ice layers with a greater water or air bubble content associated with melting morphologies (melting channels, ponds,…). During the fieldwork no clasts or fine sediment strata were found that could explain these reversed polarity bands. Behm *et al*. (2007) described similar reflection waves in the Dachstein ice cave, attributed to the existence of melt waters under the superficial frozen layers and beneath the first congelation ice layers. In Peña Castil ice block the recorded reflections may

correspond to similar morphologies (ice-filled melting morphologies)(see photos in Figure 10).

Upper congelation ice layers or pure ice layers (Behm *et al*., 2007) are imaged in the first centimetres of all radargrams and have been interpreted from the direct waves present in the GPR data. Highly homogeneous wave signals are recorded with hardly any irregularities to depths from 0,5 to 1 m (and even up to 1,5 m in some places). These signals have been interpreted as congelation ice layers that remain from the last ice accumulation period (last spring).

Conclusions

The application of GPR to the study of the Peña Castil ice block has been shown to be a useful technique for the description of its ice mass, helping us to interpret the internal structure, stratification and compaction of the topmost 7 metres using 400 MHz shielded antenna. Although basal interfaces of ice-basal bedrock contact have not been distinguished, interfaces with the bedrock walls have been observed, and the configuration of the vertical shaft-shaped cave has been determined. The ice block thickness shown in the GPR survey is consistent with estimated depth and volume of the ice block (54 m and 33,000 m^3) as has been observed in previous studies.

Several embedded clasts were detected within the ice block as well as in its surface. Although it was not possible to determine the ice block thickness to its basal bedrock, the analysis of its structure and the disposition of its strata suggest a deformation of the ice body caused by possible basal melting that could generate its vertical displacement and the strata curvature.

GPR measurements are a very useful tool with great potential in the particular case of this ice cave. The results derived will be confirmed in the future if the evolution of its ice mass provides a suitable scenario for more complete and direct visual examinations, and these outcomes offer us the possibility of determining which parts of the ice block are suitable for future research, e.g. drilling cores, necessary to making any paleoclimatological interpretation.

Acknowledgements

This research has been funded by projects I+D+I project CGL2015-68144-R (Ministerio de Economía y Competitividad) and OAPN-053/2010 (MAGRAMA) of Spanish government. We thank the “Facultad de Ingeniería en Ciencias de la Tierra de la ESPOL” for making available their georadar data processing facilities, and “Proyecto Prometeo” of “Secretaría de Educación Superior, Ciencia, Tecnología e Innovación de la República del Ecuador” for the financial support. We wish to be grateful for CES-Alpha speleological group, the assistance provided during the speleological exploration, specially to Emilio Herrera and Javier Sánchez. We are in debt with Manuel Díez and Vicente Gómez for his useful help during the field work. We are grateful to the anonymous reviewers for their helpful and suggestions. Petty Giles has helped the paper translation.

References

Achleitner A. 1995. Zum Alter des Höleneises in der Eisgruben-Eishöhle im Sarstein (Oberösterreich). *Die Höhle* **46 (1):** 1-5.

Arcone SA. 1996. High resolution of glacial ice stratigraphy: A ground penetrating radar study of Pegasus Runway, McMurdo Station, Antartica. *Geophysics* **61(6):** 1653-1663.

Behm M, Hausmann H. 2007. Eisdickenmessungen in alpinen Höhlen mit Georadar (Determination of ice thickness in alpine caves with ground penetrating radar). *Die Höhle, Zeitschrift für Karst-und Höhlenkunde* **58:** 3-11.

Behm M, Hausmann H. 2008. Determination of ice thicknesses in alpine cave using georadar. In *3rd International Workshop on Ice Caves. Proceedings*. Kadebskaya O, Mavlyudov BR, Pyatunin M (eds). Kungur, Russia; 70-74.

Behm M, Hausmann H, Weghofer C. 2010. Thickness and internal structure of underground ice in a low-elevation cave in the Eastern Alps (Beilstein-Eishöhle, Hochschwab, Austria). In *4th International Workshop on Ice Caves Abstracts Volume.* Spötl C, Luetscher M, Rittig P (eds). Obertraun, Austria; 6.

Belmonte A, Sancho C. 2010. First data from a Pyrenean ice cave (A294, Cotiella massif, Spain). In *4th International Workshop on Ice Caves*. *Abstracts Volume.* Spötl C, Luetscher M, Rittig P (eds). Obertraun, Austria; 7.

Belmonte A, Sancho C, Moreno A 2011. Chronology of a Pyrenean subsurface ice deposit (A294 cave, Cotiella massif, Spain). In *8th EGU General Assembly, Geophysical Research Abstracts*. Vienna (Austria); 13.

Belmonte A, Bartolomé M, Sancho C, Moreno A, López-Martínez J. 2012. Assessing the palaeoclimate potential of the A294 ice cave (Central Pyrenees, Northern Spain). In *5th International Workshop on Ice Cave. Abstracts Volume*. Turri S, Strini A and Tomasi F. (eds) Barzio, Valssasina, Italy; 47.

Belmonte A, Sancho C, Moreno A, López-Martínez J, Bartolomé M. 2014. Present-day environmental dynamics in ice cave A294, Central Pyrenees, Spain. *Geografia Fisica e Dinamica Quaternaria* **37:** 131-140.

Berenguer Sempere F, Gómez-Lende M, Serrano, Sanjosé Blasco J.J. 2014. Orthothermographies and 3D modeling as potential tools in ice caves studies: the Peña Castil Ice Cave (Picos de Europa, Northern Spain). *International Journal of Speleology* **43 (1):** 35-43.

Ciarletti V, Clifford S, Plettermeier D, Dorizon S, Statz Ch, Lustrementm B, Humeau O, Hassen-Khodja R, Galic A, Cais P. 2013a. Investigation of an alpine ice cave in Austria with EXOMARS WISDOM GPR. *Geophysical Research Abstracts. EGU General Assembly 2013.* Vienna, Austria.

Ciarletti V. Clifford S, Plettermeier D, Dorizon S, Statz Ch, Lustrementm B, Humeau O, Hassen-Khodja R, Galic A. 2013b. WISDOM GPR investigations of ice thickness, stratigraphy, structure and basal topography in an alpine ice cave in Dachstein, Austria. In *44th Lunar and Planetary Science Conference*, 2365-2366.

Citterio M, Turri S, Bini A, Maggi V. 2003. Some observations on the structure and morphology of an ice deposit in the “Abisso sul Margine dell’Alto Bregai” cave (Grigna Settentrionales, Italian Alps). In *6th International Symposiun Glacier Caves and Karst in Polar Regions*, Eraso A, Dominguez C (eds). Svalbard, Norway; 13-19.

Citterio M, Turri S, Bini A, Maggi, V, Stenni B, Udisti R. 2005. Chemical and stable isotopes profiles from the snow deposit in the Lo Lc 1607 ice cave (Grigna Settentrionale, Italian Alps). In *14th International Congress of Speleology, Athens*, 21-28 August 2005.

Clausen H, Vrana K, Bo hansen S, Berg Larsen L, Baker J, Siggaard-Andersen ML, Sjolte J, Lundholm SC. 2006. Continental ice body in Dobšiná ice cave (Slovakia). Part II. Results of chemical and isotopic study. In *2nd International Workshop on Ice Cave*. Turri S, Zelinka J (eds.) Demänovská Dolina, Slovak Republic, 9.

Colucci R, Forte E, Guglielmin M. 2012. Underground cryosphere in the Monte Canin massif, Alpi Giulie (Itlay). In *5th International Workshop on Ice Cave Volume Abstracts*, Turri S, Strini A, Tomasi F (eds). Barzio, Italy; 17-18.

Colucci R, Fontana D, Forte E. 2014. Characterization of two permanent ice cave deposits in the southeastern Alps (Italy) by means of ground penetrating radar (GPR). In Land L, Kern Z, Maggi V, Turri S (eds). 6th *International Workshop on Ice Cave Proceedings*. Idaho Falls, Idaho, USA; 33-39.

Del Río LM, Tejado JJ, De San José JJ, Atkinson A, Serrano E, González Trueba JJ, Fernández A. 2009. Ice match structure and depth using GPR techniques: a first approach to the Jou Negro ice patch (Picos de Europa, Spain). In *Proceeding 5th International Workshop on Advanced Ground Penetrating Radar* (IWAGPR 2009), Granada; 122-126.

Dickfoss P. 1996. Stratified ice accumulations as a source of climate proxy data. Ohio State University.

Feurdean A, Perşoiu A, Pazdur A, Onac BP. 2011. Evaluating the palaeoecological potential of pollen recovered from ice in caves: a case study from Scărişoara Ice Cave, Romania. *Review of Palaeobotany and Palynology* **165 (1-2):** 1-10.

Filipov AG. 2005. The age of the relict firn plug in the Kremeshetskaya cave, Eastern Siberia. In *Glacier Caves and Glacial Karst in High Mountains and*

Polar Regions, 7th GLACKIPR symposium Mavlyudov BR. (ed.). Institute of geography of the Russian Academy of Sciences, Moscow, 98-100.

Fórizs I, Kern Z, Nagy B, Szántó Zs, Palcsu L, Molnár M. 2004. Environmental isotope study on perennial ice in the Focul Viu Ice Cave, Bihor Mts., Romania. *Theoretical and Applied Karstology* **17:** 61-69.

Fórizs I, Perşoiu A, Kern Z, Nagy B. 2006. Stable isotope study of different water sources in Bortig ice cave, Apuseni Mts, Romania. In *2nd International Workshop on Ice Cave*. Turri S, Zelinka J. (eds.). Demänovská Dolina, Slovak Republic, May 8 - 12, 2006, 9.

Fukui K, Sone T, Strelin J, Torielli C, Mori J. 2007. Ground penetrating radar sounding on an active rock glacier on James Ross Island, Antartic Peninsula region, *Polish Polar Research* **28 (1):** 13-22

Garašić M. 2014. New research in cave Ledenica in Bukovi Vrh on Velebit Mt in Croatian Dinaric Karst. In Land L, Kern Z, Maggi V, Turri S (eds). *6th International Workshop on Ice Cave Proceedings*. Idaho Falls, Idaho, USA; 31-32.

Geczy J, Kucharovic L. 1995. Determination of the ice filling thickness at the selected sites of the Dobsinska ice cave. *Ochrana ladovych jaskyn Zilina*; 17-23.

GELL. 1995. http://www.zapespeleo.com

Gómez-Lende M, Serrano E, Sempere F. 2011. Cuevas heladas en Picos de Europa. Primeros estudios en Verónica, Altáiz y Peña Castil. *Karaitza* **19:** 56-61.

Gómez-Lende M, Serrano E. 2012a. Elementos del patrimonio geomorfológico subterráneo: las cuevas heladas de Picos de Europa (Cordillera Cantábrica). In

XII Reunión Nacional de Geomorfología. González A et al. (eds). Santander, Cantabria, España; 47-50.

Gómez-Lende M, Serrano E. 2012b. Morfologías, tipos de hielo y regímenes térmicos. Primeros estudios en la cueva helada de Peña Castil (Picos de Europa, Cordillera Cantábrica). In A*vances de la Geomorfología en España 2010-2012. Actas de la XII Reunión Nacional de Geomorfología*. González A, et al. (eds.) Santander, 17-20 September 2012: 613-616.

Gómez-Lende M, Serrano E. 2012c. First thermal, morphological and ice types studies in the Peña Castil ice cave (Picos de Europa, Cantabrian Mountains, Northern Spain In *5th International Workshop on Ice Cave. Abstracts Volume*. Turri S, Strini A and Tomasi F. (eds) Barzio, Valssasina, Italy; 52-53.

Gómez-Lende M, Berenguer F, Serrano E, Sanjosé Blasco J.J. 2013. Los ortotermogramas en los estudios de hielo de las cuevas heladas. El caso de la cueva helada de Peña Castil (Picos de Europa). In *IV Congreso Ibérico de la International Permafrost Association*. Gómez Ortiz A, et al. (eds). Núria (Vall de Ribes, España; 263-276.

Gómez-Lende M, Berenguer F, Serrrano E. 2014. Morphology, ice types and termal regime in a high mountain ice cave. First studies applying terrestrial laser scanner in the Peña Castil Ice Cave (Picos de Europa, Northern Spain*). Geografia Fisica e Dinamica Quaternaria* **37:** 141-150.

Gómez-Lende M. 2015. Las cuevas heladas en Picos de Europa: clima, morfologías y dinámicas. Tesis doctoral, Universidad de Valladolid, Valladolid;

Hausmann H, Behm M. 2011. Imaging the structure of cave ice by ground penetrating radar. *The Cryosphere* **5:** 329-340.

Holmlund P, Onac BP, Hanson M, Holmgren K, Mörth M, Nyman M. Perşoiu A. 2005. Assessing the palaeoclimate potential of cave glaciers: the example of the Scarisoara ice cave (Romania). *Geografiska Annaler*, **87 (A):** 193-201.

Hubbard B, Glasser N. 2005. Field techniques in glaciology and glacial geomorphology. John Wiley & Sons Ltd: England.

IDS-Spa (2005) Greswin software user Manual. Ingeneria dei sistema, Pisa, Italy

Kern Z, Fórizs I, Kázmér M, Nagy B, Szántó Zs, Gál A, Palcsu L, Molnár M. 2004. Late Holocene environmental changes recorded at Gheţarul de la Focul Viu, Bihor Mts, Romania. *Theoretical and Applied Karstology*, **17:** 51-60.

Kern Z, Nagy B, Surányi G, Fórizs I, Balogh D. 2006. Investigation of natural perennial ice deposits of Durmitor Mts, Montenegro. In *2nd International Workshop on Ice Cave*. Turri S, Zelinka J (eds.) Demänovská Dolina, Slovak Republic, 70-73.

Kern Z, Fórizs I, Horvatinčić N, Széles É, Bočić N, Nagy B, László P. 2006. Palaeoenvironmental record from ice caves of Velebit mountains – Ledena Pit and Vukušić Ice Cave, Croatia. In *3rd International Workshop on Ice Caves. Abstracts*. Kadebskaya O, Mavlyudov BR, Pyatunin M. (eds). Kungur, Rusia; 108-113.

Kern Z, Fórizs I, Pavuza R, Molnár M, Nagy B. 2011. Isotope hydrological studies of the perennial ice deposit of Saarhalle, Mammuthöhle, Dachstein Mts, Austria. *The Cryosphere* **5:** 291-298.

Kern Z, Széles E, Horvatincic N, Fórizs I, Bocic N, Nagy B. 2011b. Glaciochemical investigations of the ice deposit of Vukušic Ice Cave, Velebit Mountain, Croatia. *The Cryosphere* **5**: 485-494.

Kern Z, Perşoiu A. 2013. Cave ice-the inminent loss of untapped mid-latitude cryospheric palaeoenvironmental archives. *Quaternary Science Reviews* **67:** 1-7.

Lacell D. 2007. Environmental setting, (mircro) morpohologies and stable C-O isotope composition of cold climate carbonate precipitates-a review and evaluation of their potential as paleoclimatic proxies. *Quaternary Sciences Review* **26 (11-12):** 1170-1189.

Lacelle D, Lauriol B, Clark ID. 2009. Formation of sesonal ice bodies and associated cryogenic carbonates in cavern de L'Ours, Québec: kinetic isotope effects and pseudo-biogenetic crystal estructures. *Journal of caves and karst studies* **71 (1):** 48-62.

Lauriol B, Clark ID. 1993. An approach to determine the origin and age of massive ice blockages in two artic caves. *Permafrost and Periglacial Processes* **4 (1):** 77-85.

Luetscher M, Jeannin PY. 2004. A process-based classification of alpine ice caves. *Theoretical and Applied Karstology* **17:** 5-10.

Luetscher M. 2005. Processes in ice caves and their significance for paleoenvironmental reconstructions. Swiss Institute for Speleology and Karst Studies (SISKA), La Chaux-de-Fonds. Swiss.

Luetscher M, Borreguero M, Moseley GE, Spötl C, Edwards RL. 2013. Alpine permafrost thawing during the Medieval Warm Period identified from cryogenic carbonates. *The Cryosphere* **7:** 1073-1081.

Leunda M, Bartolomé M, Sancho C, Moreno A, Oliva-Urcia B, González-Sampériz P, Gil-Romera G, Gomollón A. 2015. La cueva helada de Casteret (PNOMP, Huesca): primeras aportaciones del registro de hielo. *In XIV Reunión*

Nacional de Cuaternario. Galve J.P, Azañón J.M, Pérez Peña J.V, and Ruano, P (eds.) Granada (España); 78-81.

Maggi V, Turri S, Bini A, Perşoiu A, Onac B, Stenni B, Udisti R. 2012. Two millenia of natural to antropogenic effects in Transilvana from Focul Viu ice core. In *5th International Workshop on Ice Cave.* Turri S, Strini A, Tomasi F. (eds.). Barzio, Valssasina, Italy. Sept. 16-23, 2012, Abstracts Volume, 38.

May B, Spötl C, Wagenbach D, Dublyansky Y, Liebl J. 2011. First investigations of an ice core from Eisriesenwelt cave (Austria). *The Cryosphere* **5:** 81-93.

Moorman BJ, Michel FA 2000. Glacial hydrological system characterization using ground-penetrating radar. *Hydrological Processes* **14:** 2645–2667.

Novotný L, Tulis J. 1995. Ice filling in the Dobsina ice cave. *Kras a jaskyne (Liptovsky Nikulas)*; 16-17.

Navarro FJ, Otero J, Macheret YY, Vasilenko EV, Lapazaran JJ, Ahlstrom AP, Machio F. 2009.Radioglaciological studies on Hurd Peninsula glaciers, Livingston Island, Antartica. *Annals of Glaciology* **50 (51):** 17-24

Paniagua J, Del Río M, Rufo M. 2004. Test site for the analysis to subsoil GPR signal propagation. In *Tenth International Conference on Ground Penetrating Radar Proceedings*, Slob E, Yarovoy A, Rhebergen J. (eds). Delf, Netherlands; 751-754.

Perşoiu A. 2011. Palaeoclimatic significance of perennial ice accumulations in caves: an example from Scărişoara Ice Cave, Romania. Graduate School Theses and Dissertations. University of South of Florida, USA.

Perşoiu A, Onac BP, Wynn JG, Bojar AV, Holmgren K. 2011. Stable isotope behavior during cave ice formation by water freezing in Scărişoara Ice Cave, Romania. *Journal of Geophysical Research* **116:** 1-8.

Podsuhin G, Stepanov Y. 2008. Measuring of the thickness of perennial ice in Kungur Ice Cave by georadar. In *3rd International Workshop on Ice Caves. Proceedings*. Kadebskaya O, Mavlyudov BR, Pyatunin M. (eds.) Kungur, Rusia; 52-55.

Richter DK, Riechelmann DF. 2008. Late Pleistocene cryogenic calcite spherolites from the Malachitdom Cave (NE Rhenish Slate Mountains, Germany): origin, unusual internal structure and stable C-O isotope composition. *International Journal of Speleology* **37 (2):** 119-129.

Richter DK, Meissner P, Immenhauser A, Schulte U, Dorsten I. 2010. Cryogenic and non-cryogenic pool calcites indicating permafrost and non-permafrost periods: a case study from the Hersbtlabyrinth-Advent Cave system (Germany). *The Cryosphere* **4:** 501-509.

Rojšek D. 2012. Cave ice in Velika Leden Jama V Paradani, Slovenija. In *5th International Workshop on Ice Cave Volume Abstracts*, Turri S, Strini A, Tomasi F (eds). Barzio, Italy; 19.

Sánchez J, Jordá L, Serrano E, Gómez-Lende M, Hivert B. 2011. Memoria de las exploraciones subterráneas. Macizo central de Picos de Europa, Camaleño-Cantabria. CES Alfa-AS Charentaise: Madrid.

Sancho C, Belmonte A, López-Martínez J, Moreno A, Bartolomé M, Calle M, Santolaria P. 2012. Potencial paleoclimático de la cueva helada A294 (Macizo de Cotiella, Pirineos, Huesca). *Geogaceta* **52:** 101-104.

Serrano E, Del Río M, Sanjosé JJ, González-Trueba JJ, Atkinson A, Fernández, A, Martín R. 2010. Evolución reciente y dinámica actual del helero del Jou Negro (Picos de Europa). Primera aproximación. In *Ambientes*

periglaciares, permafrost y variabilidad climática. Blanco JJ, de Pablo MA, Ramos M. (eds). Universidad de Alcalá; 39-46

Serrano E, González-Trueba JJ, Sanjosé JJ, Del Río M. 2011. Ice patch origin, evolution and dynamics in a temperate high mountain environment: the Jou Negro, Picos de Europa (NW Spain). *Geografiska Annaler* **93 (2):** 57-70.

Serrano E, González-Trueba JJ, González-García M. 2012. Mountain glaciations and paleoclimate reconstruction in the Picos de Europa (Iberian Peninsula, SW Europe). *Quaternary Research* **78:** 303-314.

Spötl C, Cheng H. 2014. Holocene climate change, permafrost and cryogenic carbonate formation: insights from a recently deglaciated, high-elevation cave in the Austrian Alps. *Climate of the Past* **10:** 1349-1362.

Stepanov Y, Tainitskiy A, Kichigin A, Kadebskaya O, Mavlyudov BR. 2014. Study of multiyear ice in Medeo cave (North Ural). In Land L, Kern Z, Maggi V, Turri S (eds). 6th *International Workshop on Ice Cave Proceedings*. Idaho Falls, Idaho, USA; 25-30.

Stoffel M, Luetscher M, Bollschweiler M, Schlatter F. 2009. Evidence of NAO control on subsurface ice accumulation in a 1200 yr old cave-ice sequence, St. Livres ice cave, Switzerland. *Quaternary Research* **72:** 16-26.

Travassos JM, Simoes JC. 2004. High-resolution radar mapping of internal layers of a subpolar ice cap, Kings George Island, Antartica. *Pesquisa Antartica Brasileira* **(4):** 57-65

Viehmann I, Silvestru E, Onac BP. 2004. Scarisoara (Romania), Eisriesenwelt, and Dachstein (Austria) ice caves: a preliminary comparative study. In *1st International Workshop on Ice Cave.* Citterio M, Turri S. (eds.). Căpuş and Scărişoara, Romania. Feb. 29 – March 3, 2004, Abstracts Volume, 31.

Vrana K, Baker J, Clusen HB, Hansen S, Zelinka J., Rufli H, Ockaik L, Janocko J. 2006. Continental ice body in Dobšiná ice cave (Slovakia)- Part I.- Project and sampling phase of isotopoic and chemical study. In *2nd International Workshop on Ice Cave*. Turri S, Zelinka J. (eds.). Demänovská Dolina, Slovak Republic, May 8 - 12, 2006, 24-28.

Žák K, Urban J, Cilek V, Hercman H. 2004. Cryogenic cave calcite from several Central European caves: age, carbon, and oxygen isotopes and a genetic model. *Chemical Geology* **206 (1-2):** 119-136.

Žák K, Onac BP, Perşoiu A. 2008. Cryogenic carbonate in cave environments: a review. *Quaternary International* **187 (1):** 84-96.

Supporting Information

Main parameters Peña Castil ice cave			
Location	Central Massif (Picos de Europa; N Spain)	Mean temperature (ice room)	-0,9 ºC
Altitude (entrance)	2095 m	Ice block surface	629 m^2
Orientation entrance	East	Estimated ice block volume	33.000 m^3
Horizontal develop.	65 m	Estimated depth ice block	-84 m
Vertical develop.	-84 m	Estimated thickness ice block	54 m

Table I. Ice cave parameters.

Typical electrical properties of ice			
Relative electrical permittivity (ε_r)	Electrical conductivity (σ) (ms m^{-1})	Velocity (V) (x10^8 ms^{-1})	Attenuation (α) (dB m^{-1})
3-4	0.01	1.67	0.01

Table II. Electrical properties of ice (from Hubbard and Glasser, 2005)

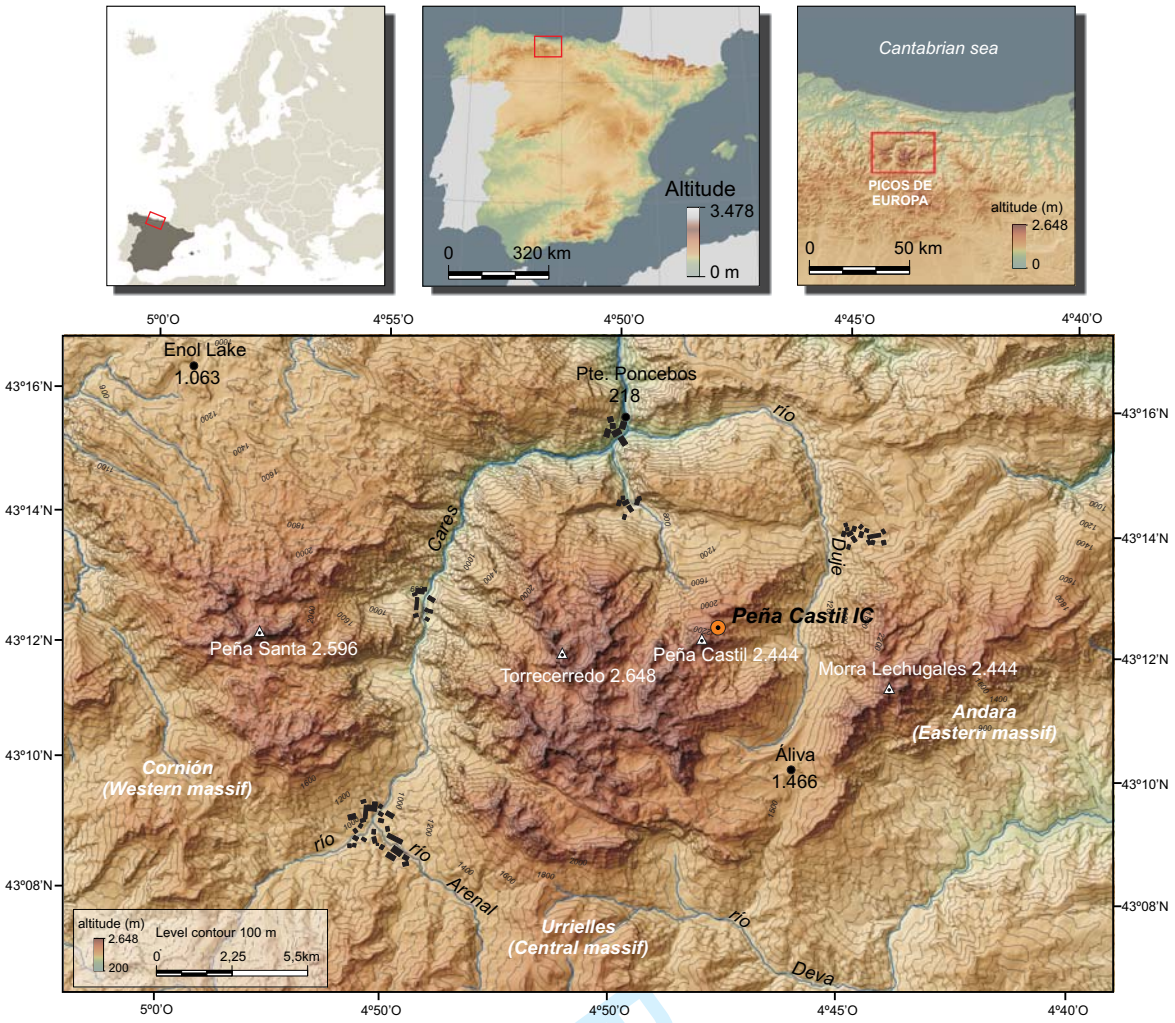
Altitude
3.478
0 m
0
320 km
Cantabrian sea
PICOS DE EUROPA
altitude (m)
2.648
0
0
50 km
5°0'O
4°55'O
4°50'O
4°45'O
4°40'O
43°16'N
43°14'N
43°12'N
43°10'N
43°08'N
Enol Lake
1.063
Pte. Poncebos
218
río
Cares
Duje
Peña Castil IC
Peña Castil 2.444
Peña Santa 2.596
Torrecerredo 2.648
Morra Lechugales 2.444
Andara
(Eastern massif)
Áliva
1.466
Cornión
(Western massif)
río
río
Arenal
Urrielles
(Central massif)
río
Deva
altitude (m)
2.648
200
Level contour 100 m
0
2,25
5,5km

PC-11

PEÑA CASTIL ICE CAVE

30T X= 354.210 Y= 4.785.460 Z= 2.095

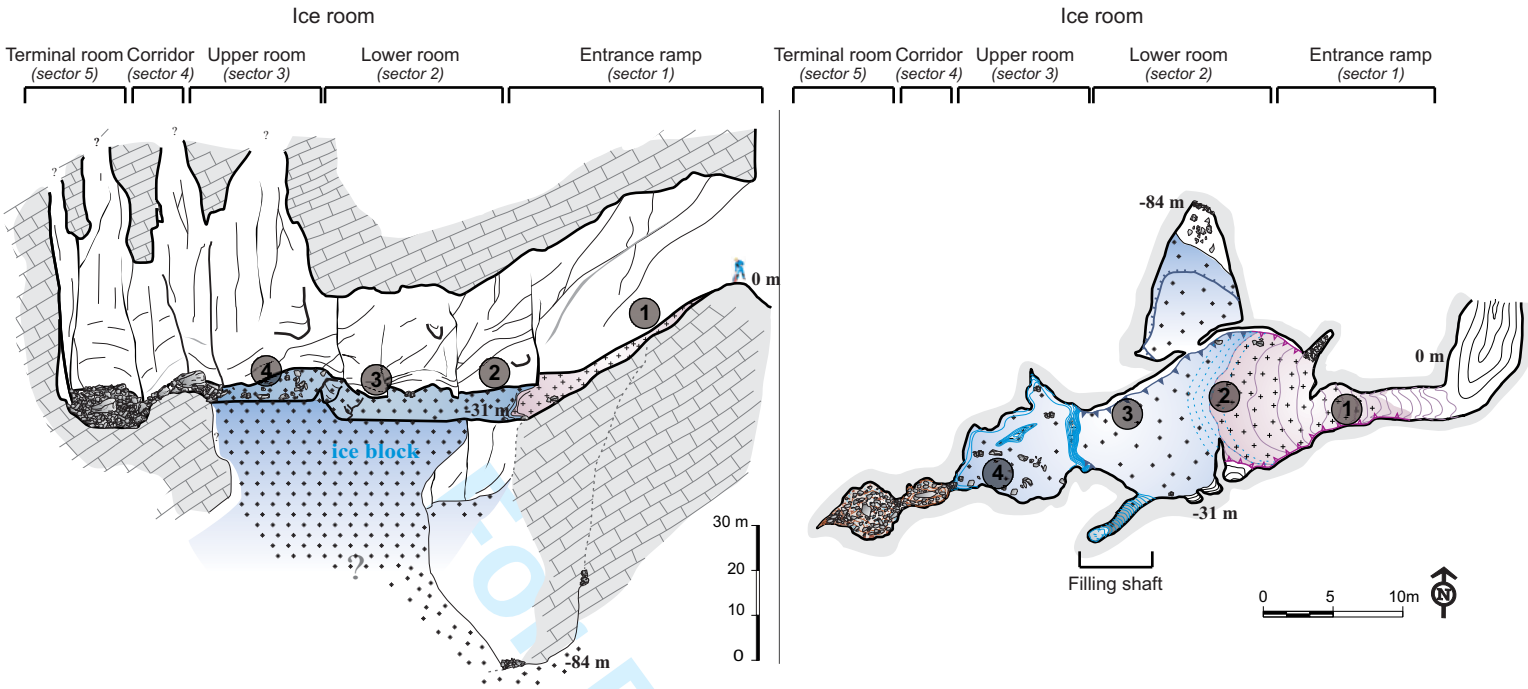

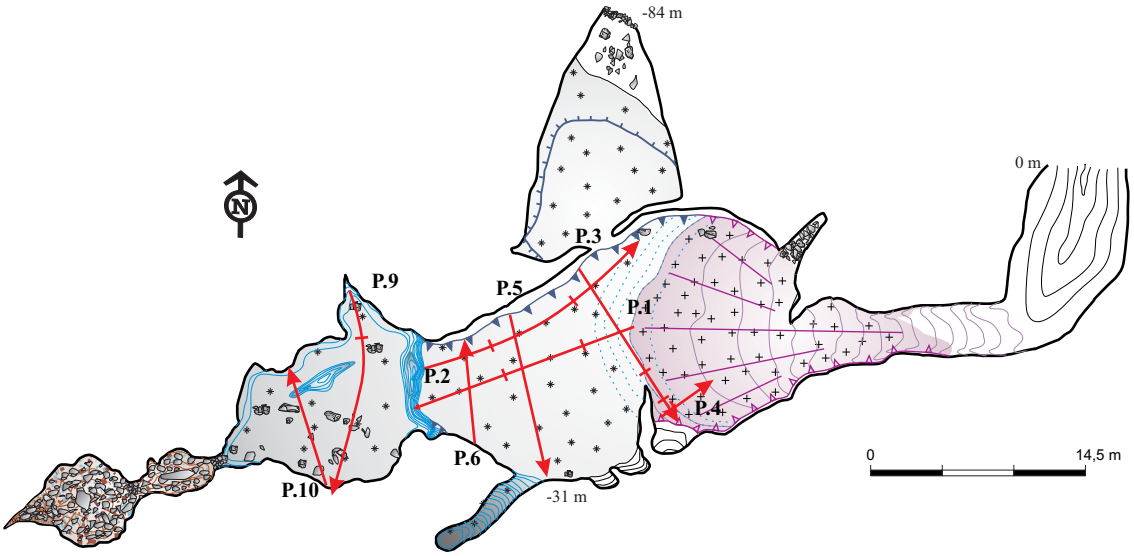

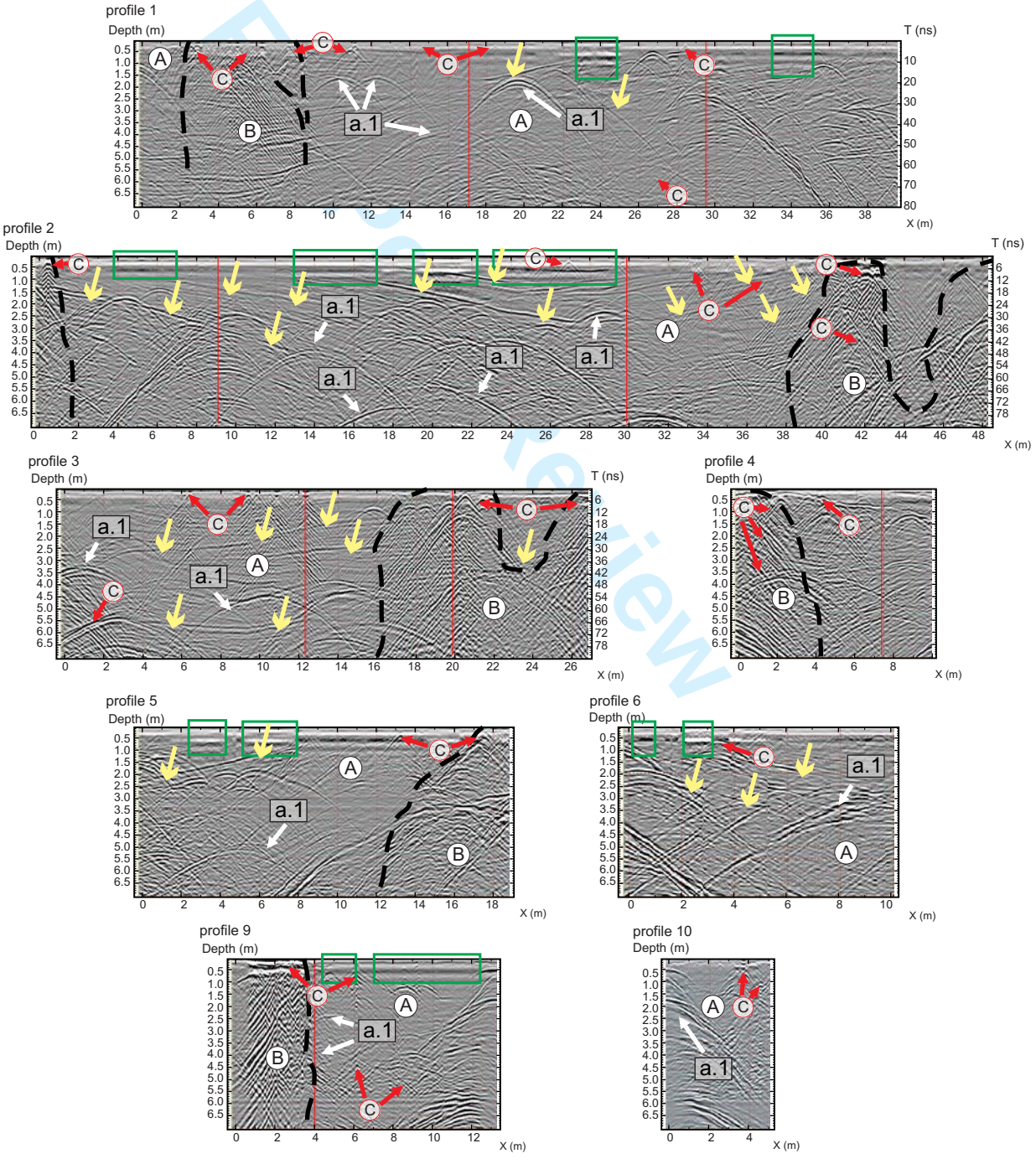

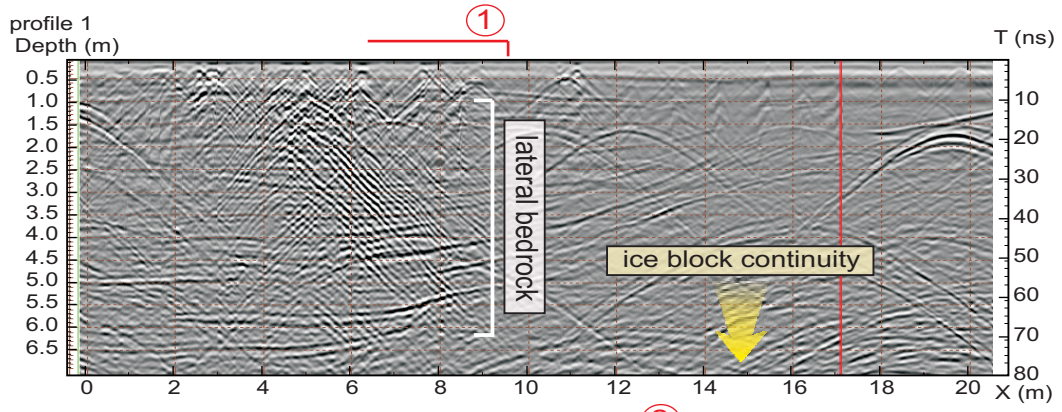
profile 1
Depth (m)
T (ns)
①
lateral bedrock
ice block continuity
X (m)

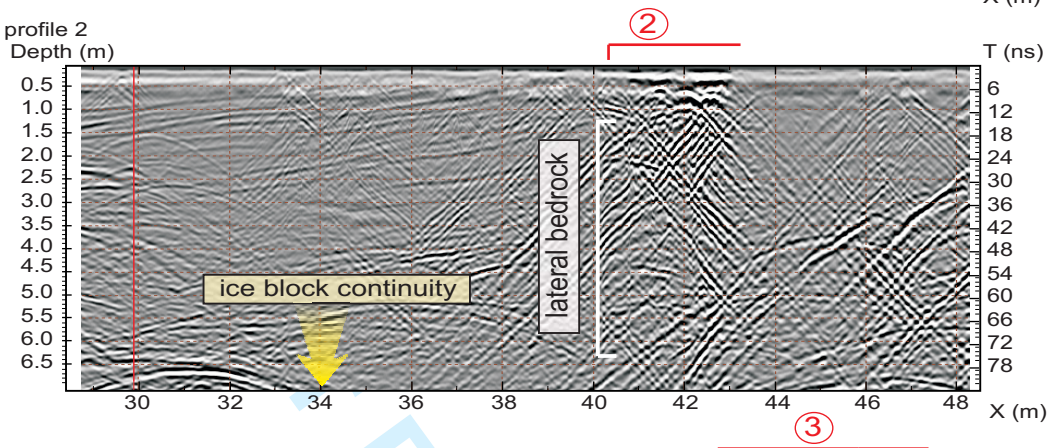
profile 2
Depth (m)
T (ns)
②
ice block continuity
lateral bedrock
X (m)

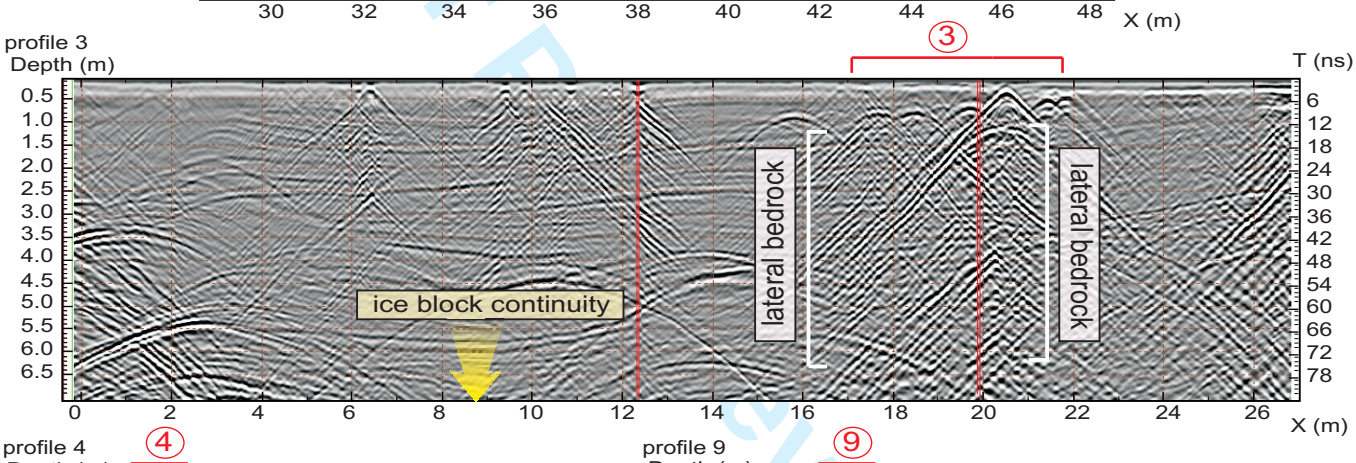
profile 3
Depth (m)
T (ns)
③
ice block continuity
lateral bedrock
lateral bedrock
X (m)

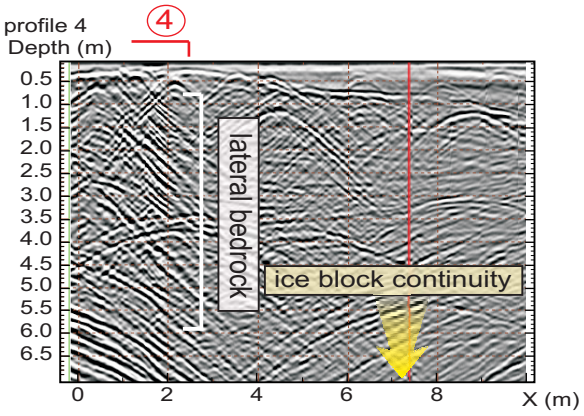
profile 4
Depth (m)
④
lateral bedrock
ice block continuity
X (m)

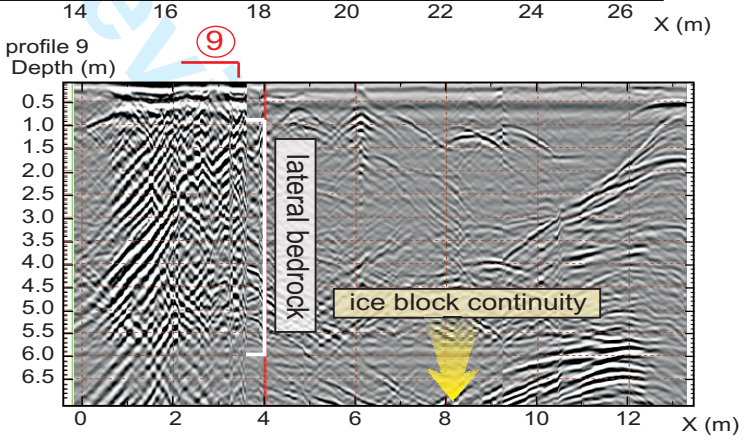
profile 9
Depth (m)
⑨
lateral bedrock
ice block continuity
X (m)

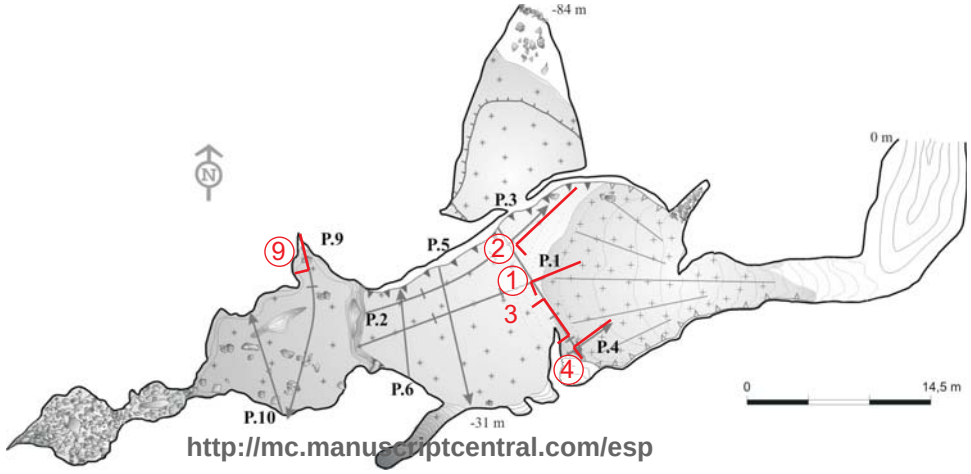
-84 m
0 m
P.3
P.9
P.5
P.1
P.2
P.4
P.6
P.10
-31 m
0
14,5 m

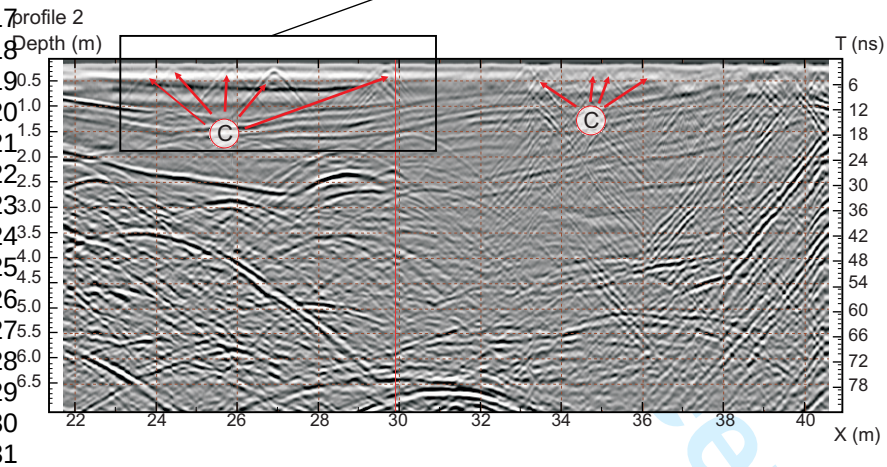

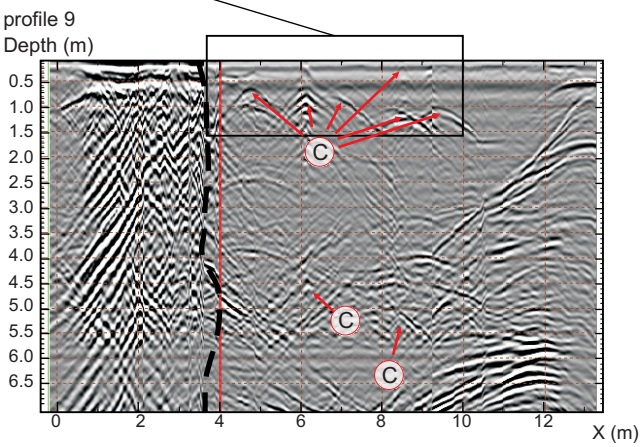

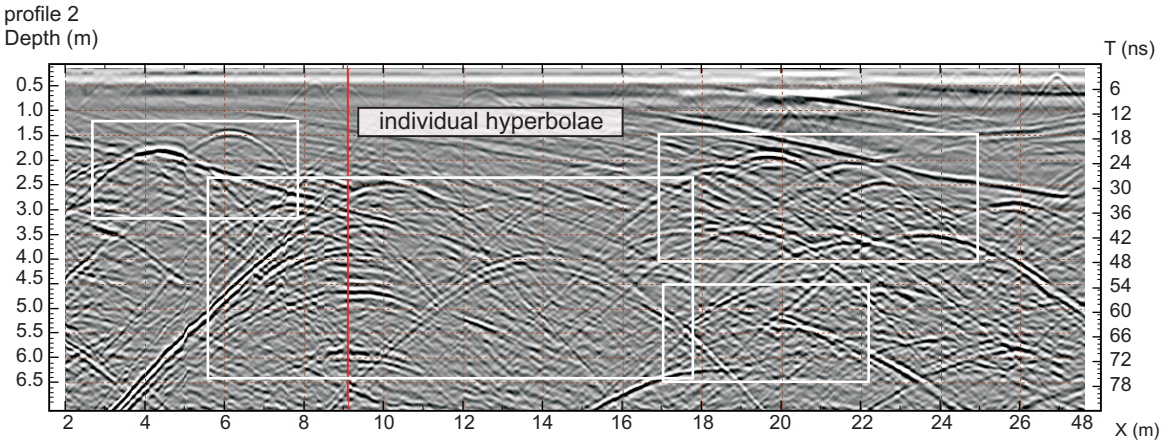
profile 2
Depth (m)
T (ns)
individual hyperbolae
X (m)

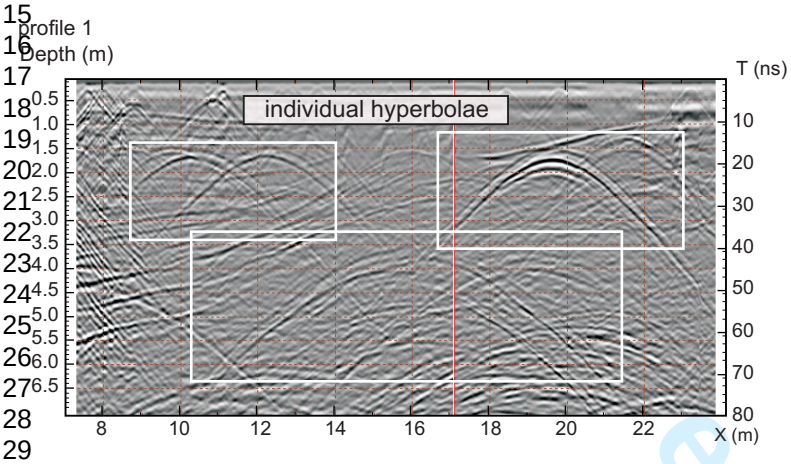
profile 1
Depth (m)
T (ns)
individual hyperbolae
X (m)

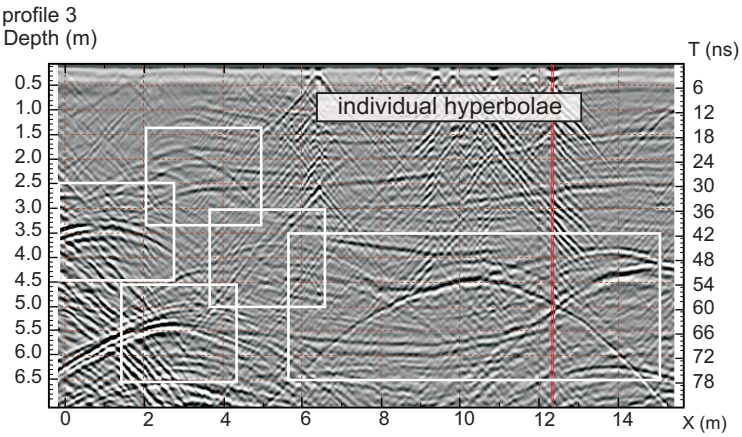
profile 3
Depth (m)
T (ns)
individual hyperbolae
X (m)

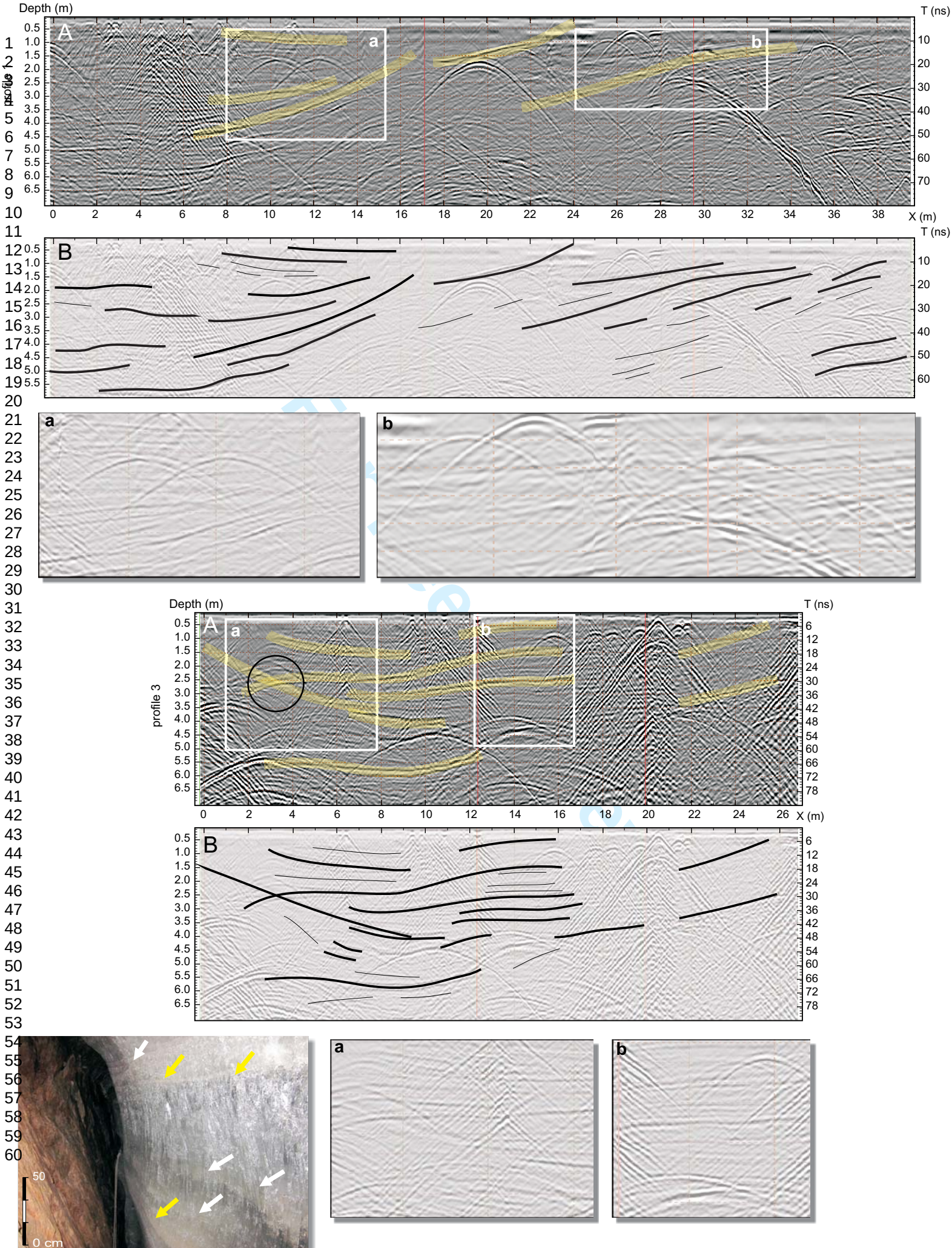
Depth (m)
T (ns)
A
a
b
profile 1
X (m)
B
a
b
Depth (m)
T (ns)
A
a
b
profile 3
X (m)
B
50
0 cm
a
b